Available online at www.CivileJournal.org

Civil Engineering Journal

Vol. 4, No. 6, June, 2018

Design and Performance of a Single Axis Shake Table and a Laminar Soil Container

Reza Alaie [a], Reza Jamshidi Chenari [b*]

[a] PhD Candidate, Department of Civil Engineering, Faculty of Engineering, University of Guilan, Rasht, Guilan, Iran.

[b] Associate Professor, Department of Civil Engineering, Faculty of Engineering, University of Guilan, Rasht, Guilan, Iran.

Received 01 April 2018; Accepted 17 June 2018

Abstract

Correct evaluation of shear modulus and damping characteristics in soils under dynamic loading is one of the most important topics in geotechnical engineering. Shaking tables are used for physical modelling in earthquake geotechnical engineering and is key to the fundamental understanding and practical application of soil behaviour. The shaking table test is realistic and clear when the response of geotechnical problems such as liquefaction, post-earthquake settlement, foundation response and soil-structure interaction and lateral earth pressure problems, during an earthquake is discussed. This paper describes various components of the uniaxial shaking table at university of Guilan, Iran. Also, the construction of the laminar shear box is described. A laminar shear box is a flexible container that can be placed on a shaking table to simulate vertical shear-wave propagation during earthquakes through a soil layer of finite thickness. Typical model tests on sandy soil conducted on the shaking table and the results obtained are also presented. Appropriate evaluation of shear modulus and damping characteristics of soils subjected to dynamic loading is key to accurate seismic response analysis and soil modelling programs. The estimated modulus reduction and damping ratio were compared to with Seed and Idriss's benchmark curves.

Keywords: Shake Table; Laminar Box; Shear Modulus; Damping Ratio; Shear Stress; Shear Strain.

1. Introduction

Natural hazards like earthquakes date from many centuries. In recent century, earthquakes all over the world have become major concern for the engineers. Having an accurate understanding of events such as site amplification, the dynamic behavior of soil and soil-structure interaction, is one of the favorite topics in geotechnical engineering seismic [1]. Several full scale and reduced scale physical and numerical models are developed and are being developed to study various problems related to geotechnical engineering. To minimize the damage due to earthquake on various structures, performance assessment of these structures under seismic loading is required. The seismic behavior of level or inclined liquefiable and soft clay grounds and soil-structure systems such as pile and shallow foundations, embankments, dams and retaining walls has been studied by the physical model tests. One of the purposes of the physical modeling is to generate data which can be used to validate numerical and analytical procedures and can be used for simulation and then extrapolating from model to the prototype scale. Kramer [2] stated that the performance of a prototype model or the effects of different parameters on geotechnical problems can be studied by model tests. Different model studies available in geotechnical engineering are: tilt table test, centrifuge test (high-g tests), hydraulic gradient tests and shaking table tests (l-g tests).

* Corresponding author: Jamshidi_reza@guilan.ac.ir

http://dx.doi.org/10.28991/cej-0309176

There are two types of geotechnical scaled seismic model tests: shaking table test at 1-g and geotechnical centrifuge testing at n-g. Some advantages of shaking table test at 1-g gravity field are its well-controlled large amplitude and easier experimental measurements in comparison to the centrifuge modelling. The main disadvantage of the shake table is the production of reduced and unrealistic stress levels. Development of high capacity actuators and enlarging the dimensions of the models is deemed to increase the stress level in shake table modelling. To facilitate testing of models of various geotechnical structures under dynamic loading conditions, University of Guila has procured a uniaxial shaking table with a laminar shear box. This paper describes the design and commissioning of the small shaking table and the laminar shear box and presents a detailed discussion of various components of the shaking table and the instrumentation developed along with typical results obtained from shaking table tests on sandy soil.

2. Shake Table Tests

Shaking table tests are one of the most important seismic model tests that has provided valuable understanding of soil-structure interaction, liquefaction, and dynamic lateral earth pressure and foundation response [2]. Wood et al. [3] provided a discussion over the application of scaling and modeling laws, the development of shear boxes for testing geotechnical systems and the control of seismic motions in shaking tables for geotechnical earthquake engineering. As the most dominating feature of earthquakes is the horizontal shaking, most of the shaking tables around the world are of uniaxial horizontal shakers. Shaking tables are usually driven by servo hydraulic actuators; their dynamic loading capacities are controlled by the capacity of the hydraulic pumps that serve the actuators. Small capacity manual shaking tables are reported by Prasad et al. [4]. Several seismic studies on shaking table are reported on various geotechnical structures and soil structure related problems namely: Kovacs et al. [5] on clay banks; Richardson and Lee [6] on reinforced earth walls; Koga and Matsuo [7] on embankments resting on liquefiable sandy ground; Orense et al. [8] on wall type gravel drains as liquefaction countermeasure for underground structures; El-Emam and Bathurst [9] on reinforced soil walls; Toyota et al [10] on flow dynamics in liquefied slope; Wartman et al. [11] on slopes; Cubrinovski et al. [12] on piles undergoing lateral spreading in liquefiable soils; Jamshidi et al. [13] on sheet pile retaining walls with fiber reinforced backfill. Sadrekarimi [14] studied soil shear modulus and damping characteristics at very shallow depths by reduced scale shaking table model experiments at small confining stresses. Araei and Towhata [15] used high-frequency GAP-sensors, accelerometers, and load cells in a laminar shear box (LSB) filled with loose Toyoura sand to understand the effects of impact loads and cyclic shaking at 1-g on soil properties. Varghese and Madhavi Latha [16] investigated the factors that influence the liquefaction resistance of sand. Having conducted a series of shaking table tests, Yong et al. [17] studied on the dynamic behavior of two selected tropical residual soils (sandy silt and silty sand) in Malaysia by applying combinations of input shaking frequencies and lateral displacements under different overburden pressures. Tsai et al. [18] investigated how the boundary effect in large specimens affects the identified soil properties through shaking table tests on a soil-filled large laminar box. Bahadori and Farzalizadeh [19] carried out a series of 1-g shaking table model tests to examine the effect of adding tyre powders and tyre shreds on the liquefaction potential of loose saturated sand and the dynamic properties of reinforced soil. Yazdandoust [20] performed a series of 1-g shaking table tests on five reduced-scale soil-nailed wall models to investigate the influence of peak acceleration, loading duration, and nail length on seismic response of the soil-nailed walls in terms of the distribution of shear modulus and damping ratio in the soil-nailed mass, the axial force distribution along the nails and the distribution of dynamic lateral earth pressure behind the wall.

3. Shaking Table Facility of University of Guilan

The computer-controlled servo electric single axis shaking table indigenously developed at University of Guilan is intended to simulate the horizontal shaking movement. The maximum weight of the models is 500 kg with a foot print of up to 1000 × 1000 mm. Shaking action is provided by a digitally controlled servo-electric actuator with 150 mm stroke and of 4.5 kW power. A pair of linear-bearings used for frictionless movement of the shaking table on loading structure at any given payload. For set up and performance testing, an input signal under constant amplitude conditions was produced by a host computer. Figure 1 shows the shaking table test facility. Various components of the shaking table facility are: loading platform, loading frame, servo-electric actuator, digital controller, application software, etc. The loading platform dimensions of shaking table are 1000 × 1000 mm that was designed for an effective loading dimension of 700 × 500 mm. Loading platform have high stiffness to weight ratio and was designed for a natural frequency in excess of 50 Hz that leads to the loading table not to resonate under dynamic loading. Loading platform with linear bearing block (Figure 2) was placed on linear rails. Linear bearings are bearings which allow free linear motion. It consists of a movable part and a guide rail. Rails were supported by steel ribs with equal support all along the travel of shaking table and the shear forces are transmitted to the base reaction frame. The loading frame was anchored to a heavy reaction mass with overall dimension of about 3 × 2.5 × 2 m and mass weighing about 35 tons. This reaction mass is approximately 70 times the moving mass, with a payload of 500 kg on loading platform.

A servo-electric actuator with a power of 4.5 kW was used for exciting the platform to a peak acceleration of 2.5g and a minimum acceleration of 0.1 g. A servo motor is a rotary actuator or motor that allows for a precise control in

terms of angular position, acceleration and velocity (Figure 2). It makes use of a regular motor and pairs it with a sensor for position feedback. The controller is the most sophisticated part of the servo motor, as it is specifically designed for the purpose. The shaft of the servo can be positioned to specific angular positions by sending a coded signal. As long as the coded signal exists on the input line, the servo will maintain the angular position of the shaft. If the coded signal changes, then the angular position of the shaft undergoes changes. A ball screw translates rotational motion of servo-actuator to linear motion. The ball screw assembly consists of a screw and a nut, each with matching helical grooves, and balls which roll between these grooves providing the only contact between the nut and the screw. As well as being able to apply or withstand high thrust loads, they can do so with minimum internal friction. They are made to close tolerances and are therefore suitable for use in situations in which high precision is necessary.

Figure 1. Shake table test facility

A digital controller was developed for test control and measurement applications, including single and multiple channel servo-controlled systems driving electromechanical, servo-electric and data acquisition. The controller is fully digitized servo control system and accepts a variety of sensor inputs including LVDT, strain bridges and digital encoders. It has 16-bit data acquisition and a digital l6 bit waveform synthesizer with sine waveforms from 0.01 Hz to 200 Hz. Host PC communication with the controller is through a USB interface, using user friendly Windows 7.0 application software. Hardware and software options are integrated for external device control. The basic software package allows the user to: set optimal data acquisition rates and record data; calibrate transducers with ease; tune the servo-response; generate custom waveforms; control access to the test system, etc. Linear variable differential transformers (LVDT) ware used to provide a continuous surveillance of the horizontal displacement of the laminar shear box. The maximum measurement range of the LVDTs is 100 mm and its resolution is 0.01 mm (Figure 3). All LVDTs are of analog voltage output type and generate continuous data to the application software as the test progresses.

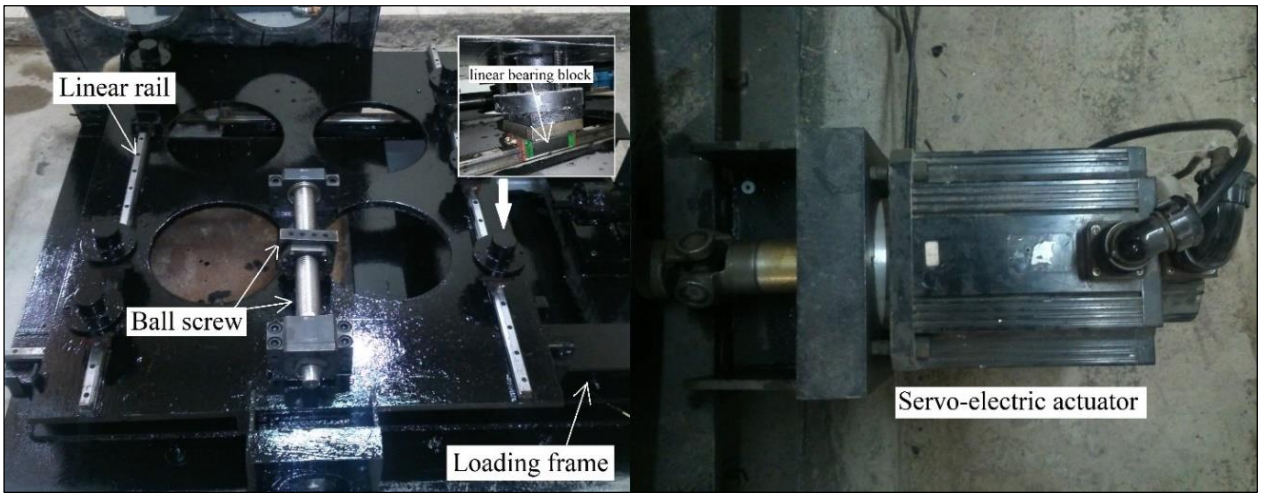

Figure 2. Various components of the shake table facility

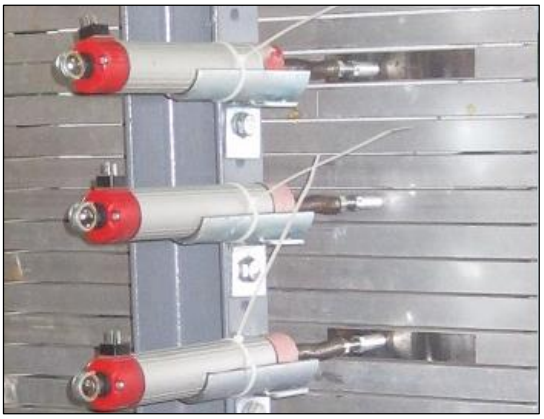

Figure 3. LVDT arrangements for external reading of the displacement mobilized in each laminar level

4. Laminar Shear Box

Influence of boundary conditions and size effect are major limitations in 1-g shaking table tests. To minimize the boundary effects on model structures, a laminar shear box was designed and built, intended to test on shaking table under dynamic conditions. The laminar shear boxes are being used since 1970s. Kokusho [21] used a 1-m deep laminar shear box for shaking table test on level fine sand model. Also, Drnevich et al. [22] used a shear box consisting of several aluminum rings in centrifuge liquefaction tests. Jamshidi chenari et al. [13] utilized a laminar shear box for investigation on dynamic properties of Toyoura sand mixed with geotextile fibers. Fiegel et al. [23] developed a new hinged plate container, composed of 4 aluminum frames which are connected to each other in the direction of the applied loads. Turan et al. [1] carried out a series of shake table tests by a laminar soil container which was developed for use in seismic soil-structure interaction studies. They studied the performance of the laminar shear box and non-linear seismic behavior of the model clay.

Figure 4 shows the laminar shear box, which was designed and manufactured at University of Guilan. The laminar shear box consists of fifteen rectangular hollow horizontal layers which are separated by ball transfer units (8 rotating ball bearing in each gap between the 2 adjacent layers) arranged to permit relative movement between the layers with minimum friction. Each gap between the 2 adjacent layers is 3 mm and the first layer from the bottom is rigidly connected to the solid steel base (Figure 5a). Ball transfer units are connected to the outside edge of the layers (Figure 5b). This ball bearing consists of one main ball having the diameter of 16 mm which has been put in a hemispherical space full of fine balls. Ball transfer units are omnidirectional load-bearing spherical balls mounted inside a restraining fixture. Typically, the design involves a single large ball supported by smaller ball bearings. Due to the low friction between layers, the movement of the layers corresponds to the movement of soil inside the shear box.

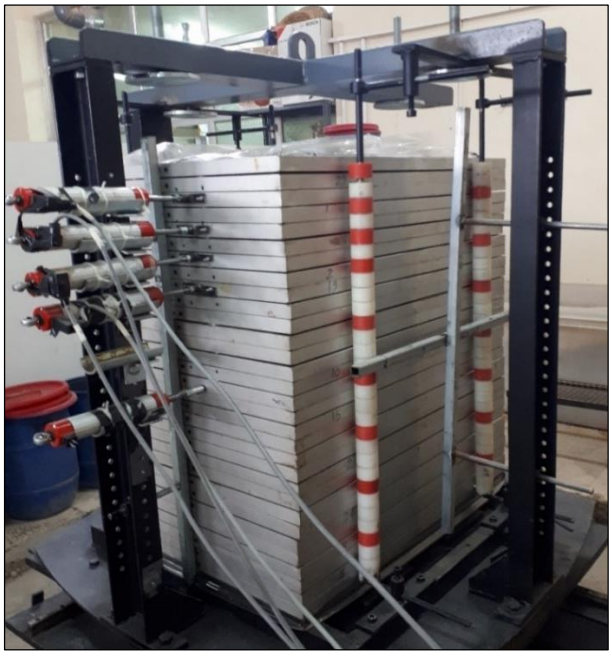

Figure. 4. Laminar shear box utilized in current study

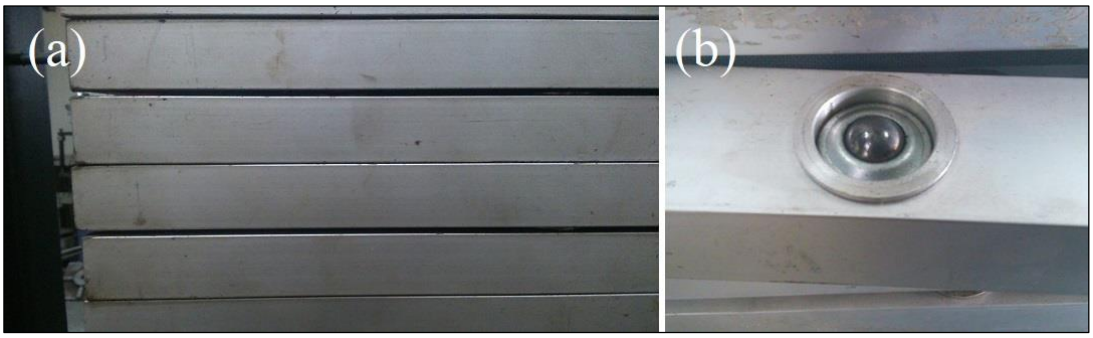

Figure 5. Laminar box system (a) the gap between successive layers (b) ball transfer units

The cross section of laminar shear box at University of Guilan is rectangular with inside dimensions of 500 × 700 and 950 mm deep. Each horizontal layer machined from solid high strength aluminum box sections (60 × 30 mm). A finite element analysis of the shear box has been done to ensure that its components remain robust and rigid during shaking table tests. In the four sides of the shear box, 4 roller columns have been installed to prevent the frames from the shaking direction while conducting the test (Figure 4). The distance of roller columns from the walls of the box is 1 mm. The thin flexible plastic membrane is used to prevent soil penetration into the gaps between laminae which also provide watertight containment in case saturated soils are tested. A wooden base plate with rough surface was used to prevent sliding at the soil-base plate interface.

5. Research Methodology

The hysteretic response of soil to cyclic shear stresses can be evaluated with reference to two fundamental parameters: shear modulus and damping factor. Each is usually expressed as a function of shear strain, γ. The variation of shear modulus and damping ratio with strain level in soil dynamics analyses are the basic input parameters. As an alternative, dynamic soil properties can be measured on a shake table using a purposely designed soil box. These parameters would ordinarily be based on element tests, however, Jamshidi et al [13] illustrated the indirect measurements and calculation of the dynamics properties of geomaterials from laminar shear box on shake table. In this paper, shake table displacement data are utilized to identify both shear modulus and damping in sandy soil. The recorded time histories of displacement from LVDT, at different depths are used to back-calculate shear stress and shear strain trails. Then, the shear modulus and damping ratio of the sand are calculated from the stress-strain data and compared with Seed and Idriss's benchmark curves.

5.1. Soil Properties and Model Preparation

The clean and uniform sand was collected from the south coast of the Caspian Sea, Iran. The grain size of the sand varied between 0.12 and 0.4 mm, with the particle size distribution curve shown in Figure 6, based on ASTM D422 [24]. According to the Unified Classification System, the sand is classified as poorly graded sand (SP) and the uniformity and curvature coefficients are 1.54 and 0.95, respectively. The specific gravity of the sand is 2.63 at a temperature of 20° C. The maximum and minimum dry unit weight of sand, γ_{dmax} and γ_{dmin}, were found to be 16.1 kN/m^3 and 14.2 kN/m^3, respectively, based on ASTM D4253 [25]. For constructing the shake table models, soil can be placed by different methods (wet or dry pluviation) to achieve uniform density or compacted and instrumented relatively easily. In order to prepare the samples while maintaining uniformity, the undercompaction moist tamping method was adopted and the sand was compacted in 9 layers from the bottom to the top of the laminar shear box. Each layer was compacted by a metal plate with dimensions of 10 ×10 cm to reach the desired relative density (55%). Before pouring the next layer, the surface of the previous layer was scratched to ensure proper bonding between consecutive layers. The above model preparation procedure was followed in order to imitate the field construction procedure as closely as possible. After preparing the complete instrumented model, the shake table is operated to apply dynamic harmonic motion and behavior of the model is observed and analyzed through physical observations and instrumental recordings. Figure 7a shows a cross-section of the laminar box and the instrumentation layout. Figure 7b shows views of the constructed laminar box models. As depicted in Figure 7a. A total of four LVDTs are used to monitor the response of the model sand deposit in the horizontal direction. A base LVDT (LVDT5) was used to measure the table motion. The fourth-order Butterworth filtering function with low-pass at 15 Hz is utilized to filter all displacement readings. The sinusoidal displacement time-histories with a frequency of 5 Hz (Figure 8) is used to study soil amplification and non-linear soil behavior with various displacement amplitudes ranging from 1 to 20 mm. Interpretation of the results is described below. To aid data processing, data acquisition was initiated a few seconds prior to the start of any shaking event and terminated. This gives flat tails to the measured time histories.

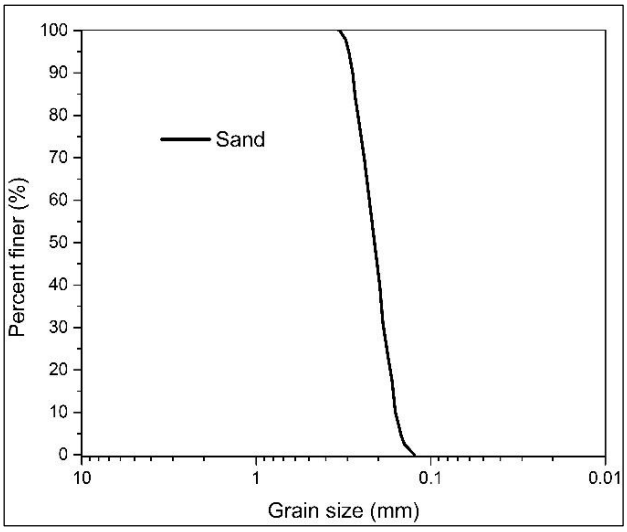

Figure 6. Sand grain size distribution curve

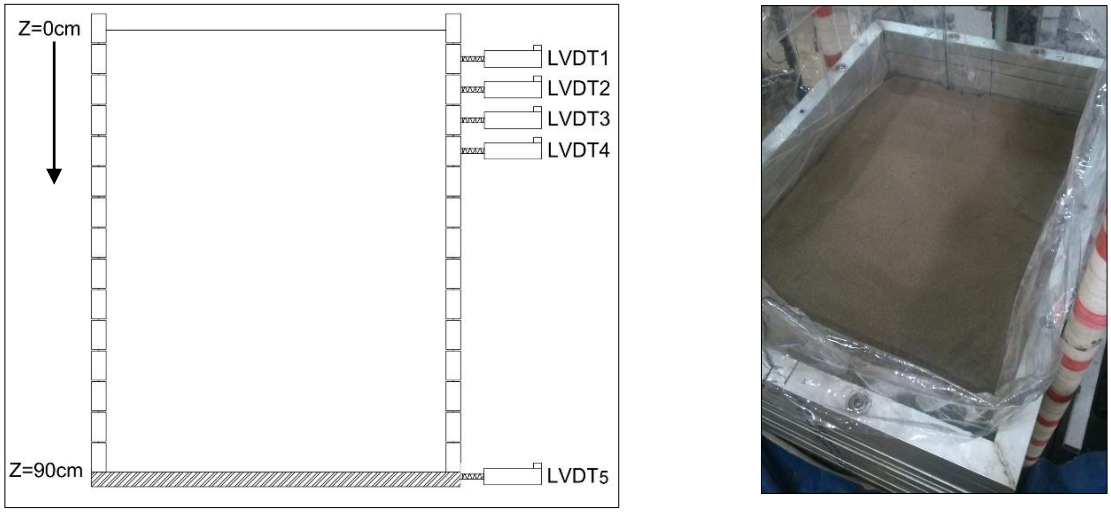

(a) **(b)**

Figure 7. Laminar box model (a) schematic of the shear box model and instrumentation (b) material inside the box

Note that laboratory cyclic tests are typically sheared at frequencies less than 1 Hz and soil shearing behaviour at $\gamma < 0.01\%$ is also captured as shearing occurs at a sufficiently slow rate. Because of the greater shaking frequency (5 Hz), the data acquisition frequency (100 Hz) of the data logger used in these model tests was not sufficient to capture the initial soil shearing behaviour at $\gamma < 0.01\%$. Also, note that the purpose of using these experimental data was to estimate dynamic properties of the model sand at small stresses, rather than a precise model of a particular prototype scale. Due to this lack of similitude, these test results are most meaningful when discussed at the model scale and no scaling is applied to transform data from the reduced-scale model tests to those of a particular prototype.

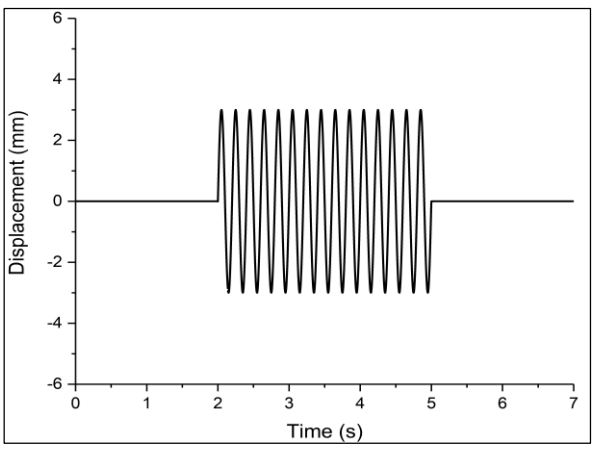

Figure 8. An example of sinusoidal loading curve

6. Evaluation of Shear Stress-Strain Histories

Data from twelve shearing events were utilized to calculate the shear stress–strain histories and estimate dynamic soil properties in terms of shear modulus and damping ratio. The shear stress and the shear strain histories at a depth of z is estimated by applying the one-dimensional shear beam model proposed by Zeghal et al. [26]. Based on 1D vertically propagating shear waves principle of the shear beam model, shear stress and shear strain response can be obtained using the lateral acceleration histories. For shear stress calculation, acceleration records were first obtained through double derivation of the corresponding recorded displacement histories. From the original shear beam equation, shear stress τ at any depth z was estimated by integrating the equation of motion at any depth as:

$$\tau(z) = \int_0^z \rho \ddot{u} dz \tag{1}$$

Where $\ddot{u}$ is the horizontal acceleration and ρ is the density. The horizontal acceleration in surface is evaluated from Equation 2. Shear stress is then evaluated using the expression of Equation 3 with the interpolated surface acceleration obtained from Equation 2 with z=0.

$$\ddot{u}(z) = \frac{\ddot{u}_1 + (\ddot{u}_2 - \ddot{u}_1)}{(Z_2 - Z_1)}(Z - Z_1) \tag{2}$$

$$\tau_i(t) = \tau_{i-1}(t) + \rho_{i-1} \frac{\ddot{u}_{i-1} + \ddot{u}_i}{2} \Delta Z_{i-1} \tag{3}$$

Where subscript *i* refers to level Z_i, $\tau_i(t) = \tau(z_i,t)$, $\tau_1(t) = \tau(0,t)=0$ at the traction-free ground surface, $\ddot{u}_i(t) = \ddot{u}(z_i,t)$, ρ_{i-1} is the average mass density for the soil layer between levels z_{i-1} and z_i, and Δz_i is the spacing interval as shown in Figure 9. The shear strain histories evaluated using Equation 4, which is equation of second order accurate shear strain at level z_i.

$$\gamma_i(t) = \frac{1}{\Delta Z_{i+1} + \Delta Z_i}\left((u_{i+1} - u_i)\frac{\Delta Z_{i-1}}{\Delta Z_i} + (u_i - u_{i-1})\frac{\Delta Z_{i-1}}{\Delta Z_i} \right) \tag{4}$$

Where $u_i = u(z_i,t)$ is the displacement data obtained from the LVDTs and Δz is the spacing between LVDTs. A compilation of the free field displacements of LVDTs for sand soil is depicted in Figure 10. Figure 11 show hysteresis loops of stress-strain behaviours of the sand. These plots illustrate nonlinear soil response and the progressive accumulation of γ with number of cycles similar to those from laboratory cyclic tests [27-29]. Figure 11 indicates that the hysteresis stress-strain loops became larger and their inclination with respect to the γ axis is decreased as γ increases, implying increased material damping and reduced soil stiffness.

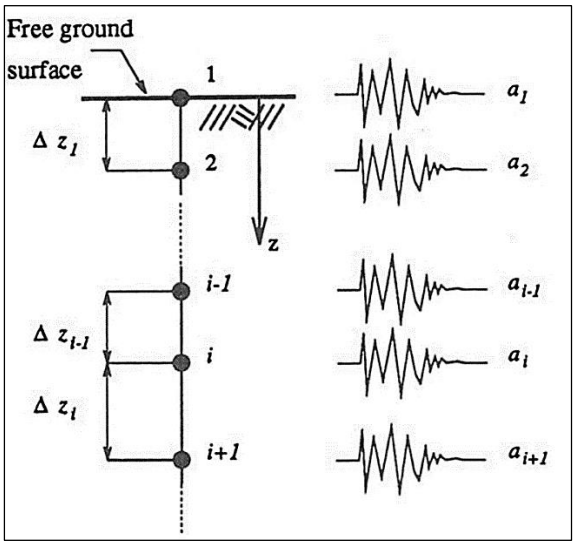

Figure 9. Soil system model and stress–strain sampling points [20]

7. Shear Modulus and Damping Ratio

The soil shear modulus and equivalent damping ratio were evaluated from the hysteresis stress-strain loops as a function of shear strain amplitude. The dynamic soil properties are calculated at different confinement levels with shear strain ranging from about 0.1 % to 1.0 %. Brennan et al. [30] has stated the rationale behind equivalent stiffness and damping and presented different methods of evaluation of shear modulus and damping in dynamic tests. Shear modulus in sand models was estimated using the secant slope of the representative shear stress–strain loop for each shaking event.

$$G_e = \frac{\tau_{\max} - \tau_{\min}}{\gamma_{\max} - \gamma_{\min}} \quad (5)$$

Back calculation of damping is performed at the stress-strain loop stage. The damping ratio was calculated from selected stress-strain loops using the area of the actual shear stress-strain loop, i.e.:

$$D = \frac{1}{4\pi}\frac{\Delta W}{W_{elastic}} = \frac{1}{4\pi}\frac{\oint \tau d\gamma}{\left(0.125\Delta\tau \times \Delta\gamma_{\max}\right)} \quad (6)$$

Where ΔW is net work, $W_{elastic}$ is the elastic work in system, $\Delta\tau$ is the total stress and $\Delta\gamma$ is the total strain range.

8. Assessment of the Shear Modulus and the Damping Ratio

In order to compare measured shear moduli with standard degradation curves, a value for the small strain shear modulus (G_{max}) is required. The G_{max} was calculated from the shear wave velocity measured using the bender element tests, i.e.

$$G_{\max} = \rho V_s^2 \quad (7)$$

Where V_s is the shear wave velocity and ρ is the soil density. Shear modulus values were normalized by the G_{max}. The shear modulus degradation curves for LVDT3 elevation are shown in Figure 12 and compared with the curves reported by Hardin and Drnevich [31] and Seed and Idriss [32] for dry fine sands. As it can be seen from Figure 12, estimated shear modulus values are close to the trends proposed by Hardin and Drenvich [31] and upper bound of Seed-Idriss [32] at high strain levels.

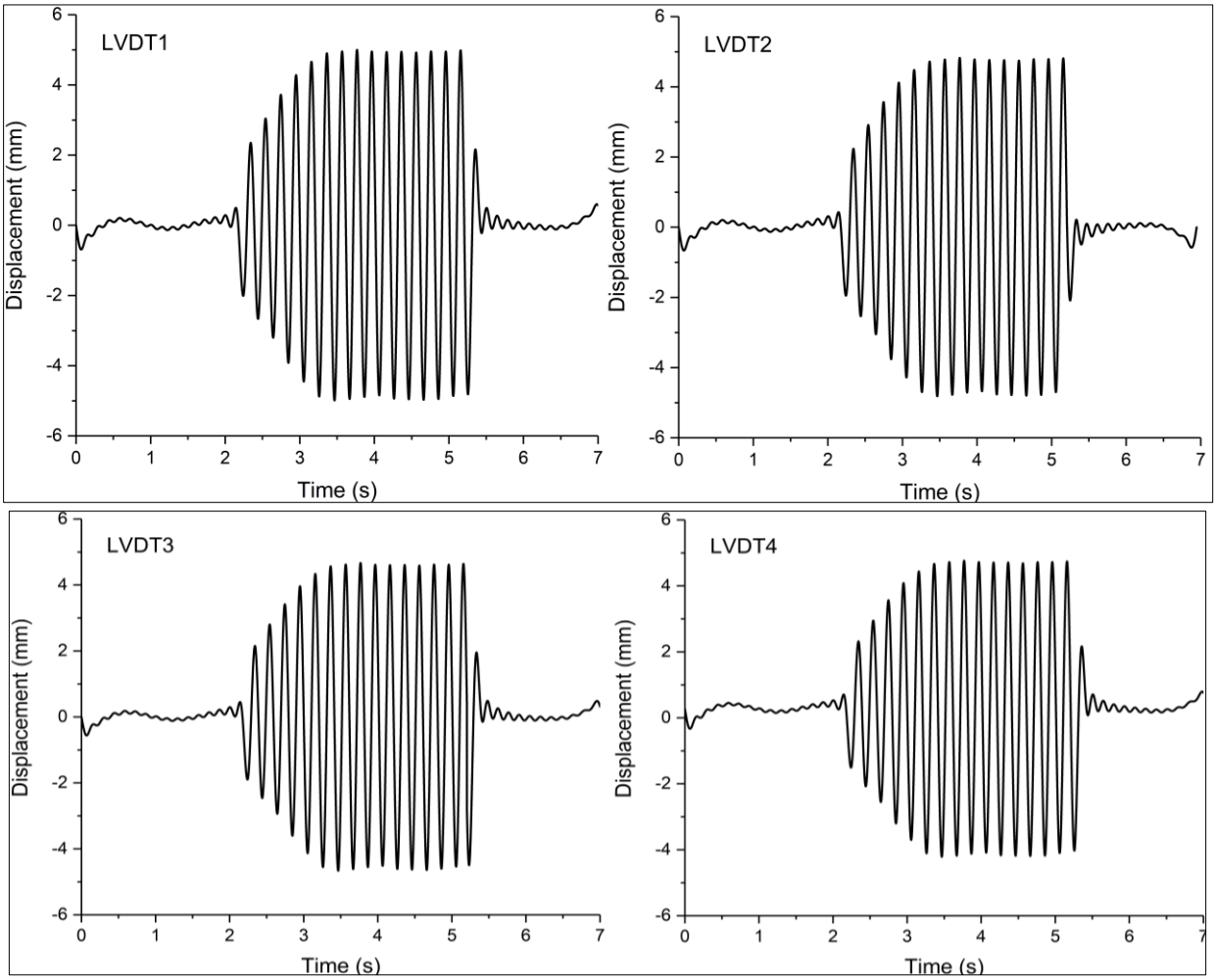

Figure 10. Representative displacement histories for 3mm displacement amplitude

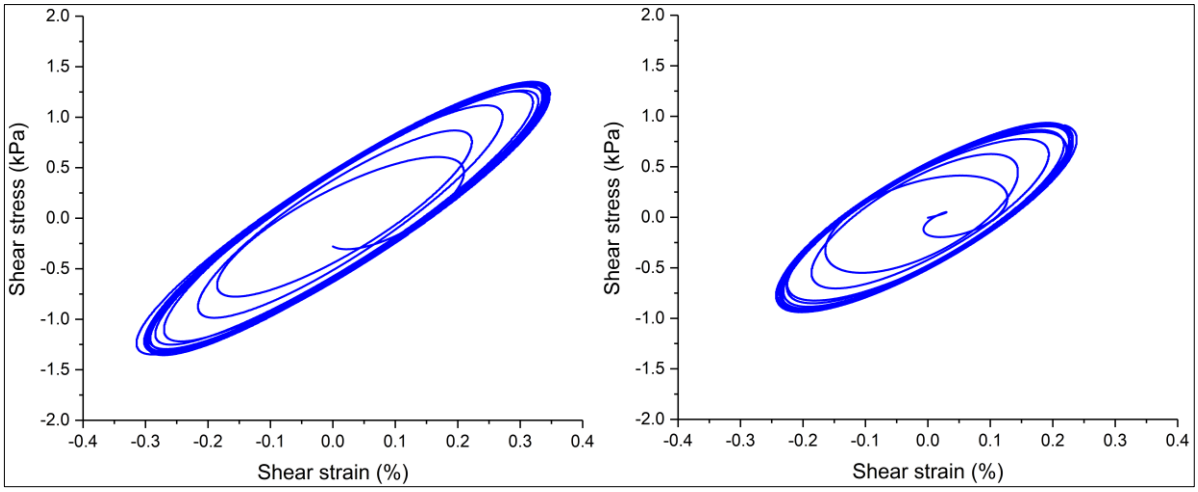

Figure 11. Shear stress–strain loops at LVDT3 level for models with 1.5 mm and 3mm displacement amplitudes

An observation from Figure 12 is that the shear modulus data pointes acquired from shake table experiments are inclined to the upper bound curve of Seed- Idriss [32]. This behavior is attributed to the densification of the sand during consecutive shaking events. The relative density of loose sand increased by about 12% after the higher amplitude shaking tests.

The damping ratio values were estimated from shear stress-strain loops during the shake table model tests. These data were compared with the damping degradation curves found in literature. Figure 13 presents the damping ratio obtained from the shake table tests along with the curves of Hardin and Drnevich [31] and Seed and Idriss [32]. In general, it is observed that the damping ratio increases with the shear strain amplitude. As it would be expected, the shake table damping ratio show low confinement behavior, in agreement with literature. Comparison of the shake table result with these of element tests shows that the damping ratio at high shear strain amplitude is slightly higher than the corresponding Hardin and Drnevich [31], Seed and Idriss [32] curves. This scatter in damping could be due to the lower confinement condition of shake table tests in comparison to the cyclic triaxial test data proposed by Hardin and Drnevich [31] and Seed and Idriss [32]. Such scatter in damping was also observed in investigation of damping such as Brennan et al. [30]. Greater scatter in the estimates of *D* is due to its sensitivity to densification, viscous damping, model boundary effects, and greater nonlinearity of sand behavior at relatively large γ (>0.01%), particularly in models with larger input base accelerations, as sand particles gained stronger contact with each other [26, 30].

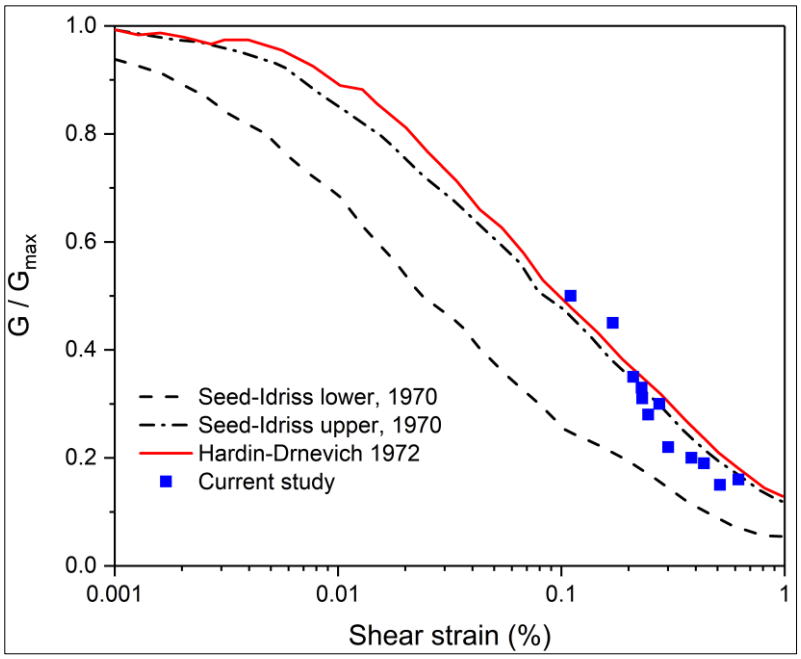

Figure 12. Shear modulus degradation of dry sand at LVDT3 elevation

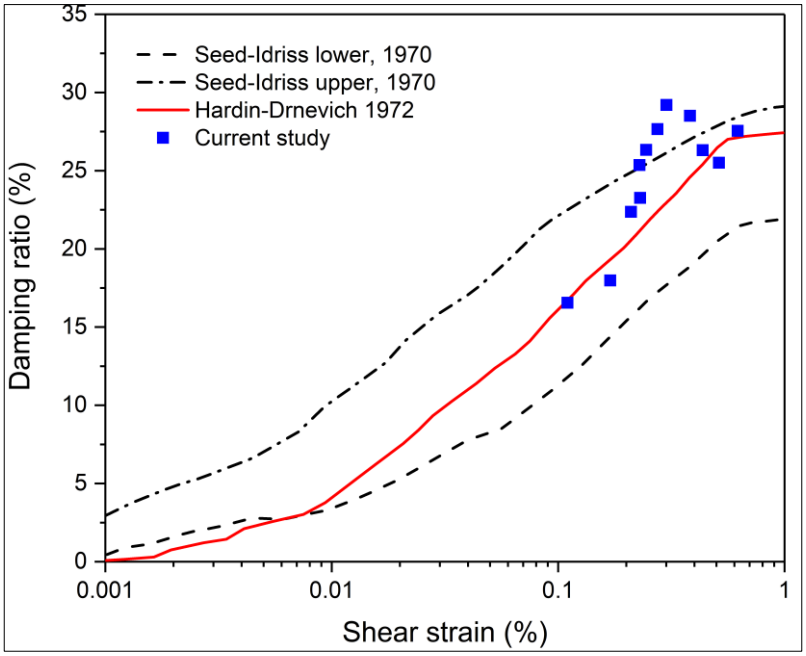

Figure 13. Calculated damping and empirical relationships for dry sand at LVDT3 elevation

9. Summary and Conclusions

There are various model tests in earthquake geotechnical engineering, this paper focus on shake table tests. The shake table and laminar box facility indigenously developed at the University of Guilan is described along with its various components and instrumentation. The whole facility can be used to test various model structures to verify and analyse the behavior of the same under a variety of dynamic loading conditions. Typical results obtained from the shake table experiments conducted on sand soil models with sine waveform motions are presented. Shake table testing of ground response for dry sand models were used to produce stress-strain data at different shear strain amplitudes. Shear stress–strain hysteresis was calculated from the displacement data, assuming one-dimensional shear beam behavior. Shear modulus and damping ratio for dry sand were estimated from the stress–strain hysteresis loops. Shear modulus data were normalized by G_{max} to obtain degradation curves and study their variation in a range of shear strain levels. The estimated shake table data were compared with those from standard design curves to evaluate the computed data for sand. In general, the shake table test results were found in reasonable agreement with the empirical trends and led to an improved confidence in the proposed curves of shake table. The evaluated shear modulus and damping ratio showed low confinement behavior in shake table models. The identified shake table modulus reduction trend seemed to be slightly higher than the conventional curves, which could be attributed to the densification of sand during dynamic successive excitations. The damping characteristics is in match with the benchmark curves found in literature for sand materials. However, a scatter was found in the damping ratio data at sand soil which was concluded to be the result of low confinement condition encountered in 1-g shake table experiments.

10. References

[1] Turan, Alper, Sean D. Hinchberger, and Hesham El Naggar. “Design and Commissioning of a Laminar Soil Container for Use on Small Shaking Tables.” Soil Dynamics and Earthquake Engineering 29, no. 2 (February 2009): 404–414. doi:10.1016/j.soildyn.2008.04.003.

[2] Kramer SL. “Geotechnical earthquake engineering” (January 7, 1996).

[3] Wood, David Muir, Adam Crewe, and Colin Taylor. “Shaking Table Testing of Geotechnical Models.” International Journal of Physical Modelling in Geotechnics 2, no. 1 (March 2002): 01–13. doi:10.1680/ijpmg.2002.020101.

[4] Prasad, S. K., I. Towhata, G. P. Chandradhara, and P. Nanjundaswamy. "Shaking table tests in earthquake geotechnical engineering." Current science (25 November 2004): 1398-1404.

[5] Kovacs, William D., H. Bolton Seed, and Izzat M. Idriss. "Studies of seismic response of clay banks." Journal of Soil Mechanics & Foundations Div (1971).

[6] Richardson, Gregory Neil. “Seismic Design of Reinforced Earth Walls.” International Journal of Rock Mechanics and Mining Sciences & Geomechanics Abstracts 12, no. 9 (September 1975): 130. doi:10.1016/0148-9062(75)91197-3.

[7] Koga, Yasuyuki, and Osamu Matsuo. “Shaking Table Tests of Enbankments Resting on Liquefiable Sandy Ground.” SOILS AND FOUNDATIONS 30, no. 4 (1990): 162–174. doi:10.3208/sandf1972.30.4_162.

[8] Orense, R.P, I Morimoto, Y Yamamoto, T Yumiyama, H Yamamoto, and K Sugawara. "Study on Wall-Type Gravel Drains as Liquefaction Countermeasure for Underground Structures." Soil Dynamics and Earthquake Engineering 23, no. 1 (January 2003): 19–39. doi:10.1016/s0267-7261(02)00152-5.

[9] El-Emam, M. M., and Richard J. Bathurst. "Experimental Design, Instrumentation and Interpretation of Reinforced Soil Wall Response Using a Shaking Table." International Journal of Physical Modelling in Geotechnics 4, no. 4 (December 1, 2004): 13–32. doi:10.1680/ijmpg.2004.4.4.13.

[10] Toyota, Hlrofumi, Ikuo Towhata, Shin-Ichi Imamura, and Ken-Ichi Kudo. "Shaking Table Tests on Flow Dynamics in Liquefied Slope." Soils and Foundations 44, No. 5 (2004): 67–84. Doi:10.3208/Sandf.44.5_67.

[11] Wartman, Joseph, Raymond B. Seed, and Jonathan D. Bray. "Shaking Table Modeling of Seismically Induced Deformations in Slopes." Journal of Geotechnical and Geoenvironmental Engineering 131, no. 5 (May 2005): 610–622. doi:10.1061/(asce)1090-0241(2005)131:5(610).

[12] Cubrinovski, M., T. Kokusho, and K. Ishihara. "Interpretation from Large-Scale Shake Table Tests on Piles Undergoing Lateral Spreading in Liquefied Soils." Soil Dynamics and Earthquake Engineering 26, no. 2–4 (February 2006): 275–286. doi:10.1016/j.soildyn.2005.02.018.

[13] Jamshidi, R., I. Towhata, H. Ghiassian, and A.R. Tabarsa. "Experimental Evaluation of Dynamic Deformation Characteristics of Sheet Pile Retaining Walls with Fiber Reinforced Backfill." Soil Dynamics and Earthquake Engineering 30, no. 6 (June 2010): 438–446. doi:10.1016/j.soildyn.2009.12.017.

[14] Sadrekarimi, Abouzar. "Dynamic Behavior of Granular Soils at Shallow Depths from 1 g Shaking Table Tests." Journal of Earthquake Engineering 17, no. 2 (May 15, 2012): 227–252. doi:10.1080/13632469.2012.691616.

[15] Aghaei Araei, Ata, and Ikuo Towhata. "Impact and Cyclic Shaking on Loose Sand Properties in Laminar Box Using Gap Sensors." Soil Dynamics and Earthquake Engineering 66 (November 2014): 401–414. doi:10.1016/j.soildyn.2014.08.004.

[16] Varghese, Renjitha Mary, and G. Madhavi Latha. "Shaking Table Tests to Investigate the Influence of Various Factors on the Liquefaction Resistance of Sands." Natural Hazards 73, no. 3 (March 21, 2014): 1337–1351. doi:10.1007/s11069-014-1142-3.

[17] Yong, Koo Kean, Lim Jun Xian, Yang Chong Li, Lee Min Lee, Yasuo Tanaka, and Zhao JianJun. "Shaking Table Test on Dynamic Behaviours of Tropical Residual Soils in Malaysia." KSCE Journal of Civil Engineering 21, no. 5 (November 11, 2016): 1735–1746. doi:10.1007/s12205-016-1856-8.

[18] Tsai, Chi-Chin, Wei-Chun Lin, and Jiunn-Shyang Chiou. "Identification of Dynamic Soil Properties through Shaking Table Tests on a Large Saturated Sand Specimen in a Laminar Shear Box." Soil Dynamics and Earthquake Engineering 83 (April 2016): 59–68. doi:10.1016/j.soildyn.2016.01.007.

[19] Bahadori, Hadi, and Roohollah Farzalizadeh. "Dynamic Properties of Saturated Sands Mixed with Tyre Powders and Tyre Shreds." International Journal of Civil Engineering 16, no. 4 (December 26, 2016): 395–408. doi:10.1007/s40999-016-0136-9.

[20] Yazdandoust, Majid. "Experimental Study on Seismic Response of Soil-Nailed Walls with Permanent Facing." Soil Dynamics and Earthquake Engineering 98 (July 2017): 101–119. doi:10.1016/j.soildyn.2017.04.009.

[21] Kokusho, Takeji. "Cyclic Triaxial Test of Dynamic Soil Properties for Wide Strain Range." Soils and Foundations 20, No. 2 (1980): 45–60. doi:10.3208/sandf1972.20.2_45.

[22] Drnevich, VP, RV Whitman, and PC Lambe. "Effect of Boundary Conditions upon Centrifuge Experiments Using Ground Motion Simulation." Geotechnical Testing Journal 9, no. 2 (1986): 61. doi:10.1520/gtj11031j.

[23] Fiegel, Gregg L., and Bruce L. Kutter. "Liquefaction Mechanism for Layered Soils." Journal of Geotechnical Engineering 120, no. 4 (April 1994): 737–755. doi:10.1061/(asce)0733-9410(1994)120:4(737).

[24] ASTM, D. 422. "Standard test method for measurement of particle size analysis of soils." ASTM, Philadelphia, Pennsylvania, USA (2004).

[25] ASTM, D. 4253. "Standard test method for maximum index density and unit weight of soils using a vibratory table." Annual Book of ASTM Standards. American Society for Testing and Materials, West Conshohocken, PA (2002): 1-14.

[26] Zeghal, M., A-W. Elgamal, H. T. Tang, and J. C. Stepp. "Lotung Downhole Array. II: Evaluation of Soil Nonlinear Properties." International Journal of Rock Mechanics and Mining Sciences & Geomechanics Abstracts 33, no. 1 (January 1996): A21. doi:10.1016/0148-9062(96)87504-8.

[27] Wichtmann, T., A. Niemunis, and Th. Triantafyllidis. "Strain Accumulation in Sand Due to Cyclic Loading: Drained Cyclic Tests with Triaxial Extension." Soil Dynamics and Earthquake Engineering 27, no. 1 (January 2007): 42–48. doi:10.1016/j.soildyn.2006.04.001.

[28] Díaz-Rodríguez, J. A., V. M. Antonio-Izarraras, P. Bandini, and J. A. López-Molina. "Cyclic Strength of a Natural Liquefiable Sand Stabilized with Colloidal Silica Grout." Canadian Geotechnical Journal 45, no. 10 (October 2008): 1345–1355. doi:10.1139/t08-072.

[29] Wijewickreme, Dharma, Ali Khalili, and G. Ward Wilson. "Mechanical Response of Highly Gap-Graded Mixtures of Waste Rock and Tailings. Part II: Undrained Cyclic and Post-Cyclic Shear Response." Canadian Geotechnical Journal 47, no. 5 (May 2010): 566–582. doi:10.1139/t09-122.

[30] Brennan, A. J., N. I. Thusyanthan, and S. P. Madabhushi. "Evaluation of Shear Modulus and Damping in Dynamic Centrifuge Tests." Journal of Geotechnical and Geoenvironmental Engineering 131, no. 12 (December 2005): 1488–1497.

doi:10.1061/(asce)1090-0241(2005)131:12(1488).

[31] Hardin, Bobby O., and Vincent P. Drnevich. "Shear modulus and damping in soils: design equations and curves." Journal of Soil Mechanics & Foundations Div 98, no. sm7 (1972).

[32] Seed, H. B. and Idriss, I. M. "Soil Moduli and Damping Factors for Dynamic Response Analysis". Report No. EERC 70-10, University of California, Berkeley, (December 1970).